

Two new cyclosporin folds observed in the structures of the immunosuppressant cyclosporin G and the formyl peptide receptor antagonist cyclosporin H at ultra-high resolution

Brian Potter,^a Rex A. Palmer,^{*a} Robert Withnall,^b Terence C. Jenkins^c and Babur Z. Chowdhry^{*b}

^a School of Crystallography, Birkbeck College, University of London, Malet Street, London, UK WC1E 7HX

^b School of Chemical and Life Sciences, University of Greenwich, Medway Campus, Central Avenue, Chatham Maritime, Kent, UK ME4 4TB

^c YCR Laboratory of Drug Design, Tom Connors Cancer Research Centre, University of Bradford, Bradford, West Yorkshire, UK BD7 1DP

Received 14th October 2002, Accepted 4th March 2003

First published as an Advance Article on the web 1st April 2003

Cyclosporins are cyclic undecapeptides of fungal origin the best known of which, CsA, is a lead clinical immunosuppressant; CsG is a potential clinical immunosuppressant differing from CsA in residue 2 (L- α -amino-butyric acid in CsA, L-norvaline in CsG); and CsH is an inverse formyl peptide receptor agonist, differing from CsA in the chiral inversion of MeVal-11 from L to D. Crystal structure determinations of CsG and CsH were undertaken to identify structural and surface features important for biological activity and the future design of new cyclosporin derivatives. Ultra-high resolution X-ray structures (0.80 to 0.87 Å resolution) determined for two crystal forms of both CsH and CsG in the presence and absence of Mg²⁺ are described. A major outcome of this study is the observation that the local change in chirality between CsA and CsH is associated with a major structural transformation from open β -sheet in CsA to a highly convoluted conformation in CsH. CsG also possesses a completely novel cloverleaf motif with no H-bonded secondary structure features in spite of the minimal chemical difference with CsA. Unlike CsA, the structures of both CsH and CsG are heavily solvated. This study therefore shows that the chemical differences between the three cyclosporins, CsA, CsG and CsH can invoke unpredictably major differences in their 3D structures. The 9–11 *cis*-peptide bond in CsA moves to 11–1 in CsG, influencing the overall molecular conformation, while the peptide bonds in the highly convoluted loop conformation of CsH are all *trans*.

Introduction

In contemporary medicine many compounds obtained from fungal sources are either being used (*e.g.* cyclosporin A, rapamycin and FK506) or actively investigated [*e.g.* cyclosporin G (CsG) and mycophenolate mofetil] as potentially useful clinical immunosuppressive agents. Engineered monoclonal antibodies and other peptide/protein ligands are currently also being developed as next-generation immunosuppressants.¹ Cyclosporins have important clinical applications, usually in combination with other therapeutic agents, in human kidney, heart and liver transplantation and increasingly in transplants of bone marrow, lung, heart/lung and pancreas.

Cyclosporin A (CsA) is a neutral and extremely hydrophobic cyclic undecapeptide (1-octanol/water partition ratio = 120 : 1) of fungal origin in which, unusually, seven of the eleven amino acids are *N*-methylated. For the past twenty years, CsA has been widely used clinically as one of the key drugs used in the prevention and treatment of graft rejection following organ and tissue transplantation.² The fungus *Beauveria nivea* produces 25 known different cyclosporins with amino acid modifications at all positions except the conserved sarcosine at position 3 of CsA. Cyclosporins are synthesised, *in vivo*, by a non-ribosomal pathway *via* the enzyme cyclosporin synthetase. Other fungi also synthesise analogous compounds. Non-ribosomally synthesised peptides from bacteria and fungi frequently contain *N*-methylated amino acids, which have a greater propensity to adopt the *cis* rather than *trans* conformation. Interestingly, *cis* amide bonds are uncommon in ribosomally synthesised mammalian proteins.

Recently several chemical modifications of the naturally occurring cyclosporins have been tried in attempts to modulate the immunosuppressive activity and other pharmacological properties of these cyclic peptides.^{3,4} Furthermore, CsA and CsG have been proposed for use in the treatment of psoriasis.⁵ Consequently structure-based⁶ and structure-function⁷ relationships for cyclosporins are currently of wide and significant interest. CsA is known to function by binding to the intracellular protein, cyclophilin (CyP), forming a CyP–CsA complex that inhibits the phosphatase activity of the Ca²⁺/calmodulin-regulated serine/threonine-specific protein phosphatase, calcineurin.⁸ CyPs also possess peptidyl–prolyl isomerase activity and can promote the *in vivo* re-folding of proteins. However, this enzyme activity appears to be unrelated to molecular mechanisms of cyclosporin immunosuppression.

The conformation of CyP-bound CsA is very different from the dominant structure adopted by free CsA either in single crystals or in solvents such as chloroform. In the complex, all the CsA peptide bonds are *trans* and none of the four intramolecular H-bonds are identified from the free structure. A single intramolecular H-bond exists between the hydroxyl group on the Bmt-1 side-chain and carbonyl oxygen atom of MeLeu-4. This conformation has been observed in solution by NMR⁹ and in the solid state in two different crystal forms.¹⁰ In addition, only CsA residues 9–11 and 1–3 are in contact with CyP. The other amino acid residues (4–8) protrude out from the CyP surface and are implicated in specific protein interactions with calcineurin. The structures for CyP complexed with eleven different CsA derivatives have been reported.¹¹ Derivatives of CsA with structural changes in amino acid residues 9–11, 1 and 2

were found to have modified binding characteristics toward CyP, which apparently correlate with changes in immunosuppressive activity. However, structural modifications of amino acid residues 4–6 also influence this activity without significantly altering the binding to CyP. The structural results suggest that CsA must have a particular solution conformation before it can bind to CyP. The crystal structure of a CsA analogue, peptiolide-214103, has also been determined in both the free form and as the CyP-bound complex.¹² Peptiolide-214103 differs from CsA in that the amino acids in positions 2, 5, 8 and 10 of CsA (Abu-2, Val-5, D-Ala-8 and MeLeu-10) are replaced by threonine-2, leucine-5, D-2-hydroxyisovaleric acid-8 and leucine-10, respectively. The CyP-peptiolide-214103 and CyP-CsA complexes are closely similar in structure whilst the conformations of the free CsA and peptiolide-214103 are very different.

The solid state X-ray structure of CsA crystallized from chloroform apparently shows a very similar conformation to that determined by ¹H and ¹³C NMR spectroscopy of CsA in chloroform solution.^{13,14} Several crystal forms of CsA and derivatives, crystallized from a range of solvents, including ethanol, ether and acetone, have also been examined and in most cases the conformation is very similar.¹⁵ Whereas CsA has high affinity for CyP, the analogue CsH, the three-dimensional structure of which is reported here, has extremely low affinity⁸ and is devoid of immunosuppressive activity. Similarly, both CsA and CsG display antifungal activity but the CsH variant does not. Many crystallographic (X-ray and neutron diffraction) and spectroscopic (NMR) structural studies of CsA and its complex with cyclophilin have appeared,^{9–19} however, no high-resolution structural data are available for either CsG or CsH.

CsH has been widely used to investigate a wide spectrum of biological phenomena. Interestingly, some of the interactions of CsA and CsH with endogenous biomolecular systems in mammalian systems are similar whilst others are unique to CsH. Importantly, CsH is an inverse formyl peptide receptor (FPR) agonist²⁰ which stabilises the FPR in an inactive state (normally the human FPR possesses high constitutive activity and couples to pertussis toxin-sensitive G_i proteins to activate chemotaxis and exocytosis in neutrophils). CsA does not display an interaction with FPR, and equivalent data for CsG are unavailable. Other biological processes which have been investigated using CsH include apoptosis,²¹ functional expression of potassium channels, cancer and HIV research, calcium potentiating effects in vascular smooth muscle, nitric oxide synthase activity,²² and virus-induced cell fusion.²² Furthermore, CsH is often employed as a reference peptide for studies of the biological activity of CsA and other immunosuppressants.²³

We describe here the crystal structures of CsH and CsG determined to better than 0.9 Å resolution. This work provides the first high-resolution structures of these peptides and allows a comparison to be made with the previously reported structure of CsA. Properties of the molecular surfaces have been calculated and their details compared.

Results

We describe here the results of crystal structure analyses for both CsH and CsG in two crystal forms, which differ in that form II is grown in the presence of Mg(ClO₄)₂. Both CsH and CsG proved to be difficult to crystallize, but in each case, as shown here, Mg(ClO₄)₂ provided a stabilizing effect on the more mobile side-chains. Although structural Mg(ClO₄)₂ does not occur in any of the crystals the presence of both Mg and Cl was detected using energy dispersive X-ray fluorescence spectroscopy.

Overall structure of CsH forms I and II

CsH forms I and II both adopt the same highly convoluted figure-of-eight secondary structure (Fig. 1a). There is only one

chemical difference between CsA and CsH, that is the L to D inversion of MeVal-11, and this is now shown to be associated with the significant structural transformation from a fairly open, mainly β-sheet structure in CsA (Fig. 1c)^{14,15} to the highly twisted conformation now observed in CsH. Nevertheless the extent of the structural changes would be difficult to predict theoretically. In addition there are significant differences in the circular dichroism spectra of CsA and CsH (Chowdhry *et al.*, to be published). Of the several solvation water molecules O1W is extremely well ordered as judged by the refined anisotropic displacement parameters (however, consideration of its interactions with neighbouring atoms rules out the possibility that this could be a co-ordinated Mg²⁺ cation).

Overall structure of CsG forms I and II

CsG crystals diffract X-rays very weakly at room temperature. Structures of both forms I and II were therefore obtained at liquid N₂ temperatures. A remarkable structural difference is observed between CsG forms I/II (Fig. 1b) and CsA (Fig. 1c). CsG adopts a compact clover leaf trefoil conformation which bears no resemblance to either the classical open β-sheet structure in CsA,^{14,15} or the novel CsH conformation described in this paper. The only difference between the primary structures of the amino acid residues of CsA and CsG is the presence of an extra methylene group in the unbranched side-chain of the L-Nva-2 residue of CsG compared to L-Abu-2 of CsA. The global structural differences which accompany this change would be difficult to predict with confidence *a priori*.

Differences in polypeptide conformation are quantified in the composite Ramachandran plots in Fig. 2a (CsA and CsH) and 2b (CsA and CsG). Table 1 lists the principal secondary structure features of CsA, CsH and CsG with selected key intra-chain distances for comparison. Fig. 3 depicts the hydrogen bonding scheme of the secondary structure of CsA^{14,19} and water, together with those of CsH and CsG for comparison. A comparison of the dihedral angles (ϕ and ψ) of the CsA structure with those of the CsH and CsG structures is shown in Table 2. †

Comparison of CsA and CsH folding

The composite Ramachandran plot of Fig. 2a shows the observed ϕ, ψ angles of CsA and CsH that enables a visualisation of the conformational changes. The average absolute change in ϕ is 37° and 56° in ψ (Table 2). Major variations in both ϕ and ψ for a given residue occur infrequently, being greatest for residue 6 with changes of 146° in ϕ and 115° in ψ , respectively. Residue 8 is the only other residue which has undergone a change in ψ greater than 36°; all residues except 10 have experienced changes in ψ greater than 15°. For the CsH structure we therefore conclude that changes in ψ are the dominant feature in the conversion from the CsA conformation. A further major difference in main-chain conformation between the CsA structure and CsH occurs at L-MeLeu-9, where the peptide bond geometry in CsA is *cis* ($\omega = 3^\circ$),^{14,19} but the usual *trans* conformation ($\omega = -166^\circ$) is adopted in CsH. The energy required for the *cis-trans* transition is about 5 kcal mol⁻¹, and this change of conformation in the main chain is certainly associated with some of the other changes in structure observed here.

† As stated above, the structural metamorphoses now observed in the crystal structures of CsH and CsG, compared to the classical CsA structure, would be difficult to predict with confidence without prior knowledge of the two structures. However we have established using extended dynamics simulation methods (SYBYL 6.4 program, Tripos UK Ltd) that thermal-induced interconversion of the backbone conformations is possible for all three structures. Full details will be published elsewhere.

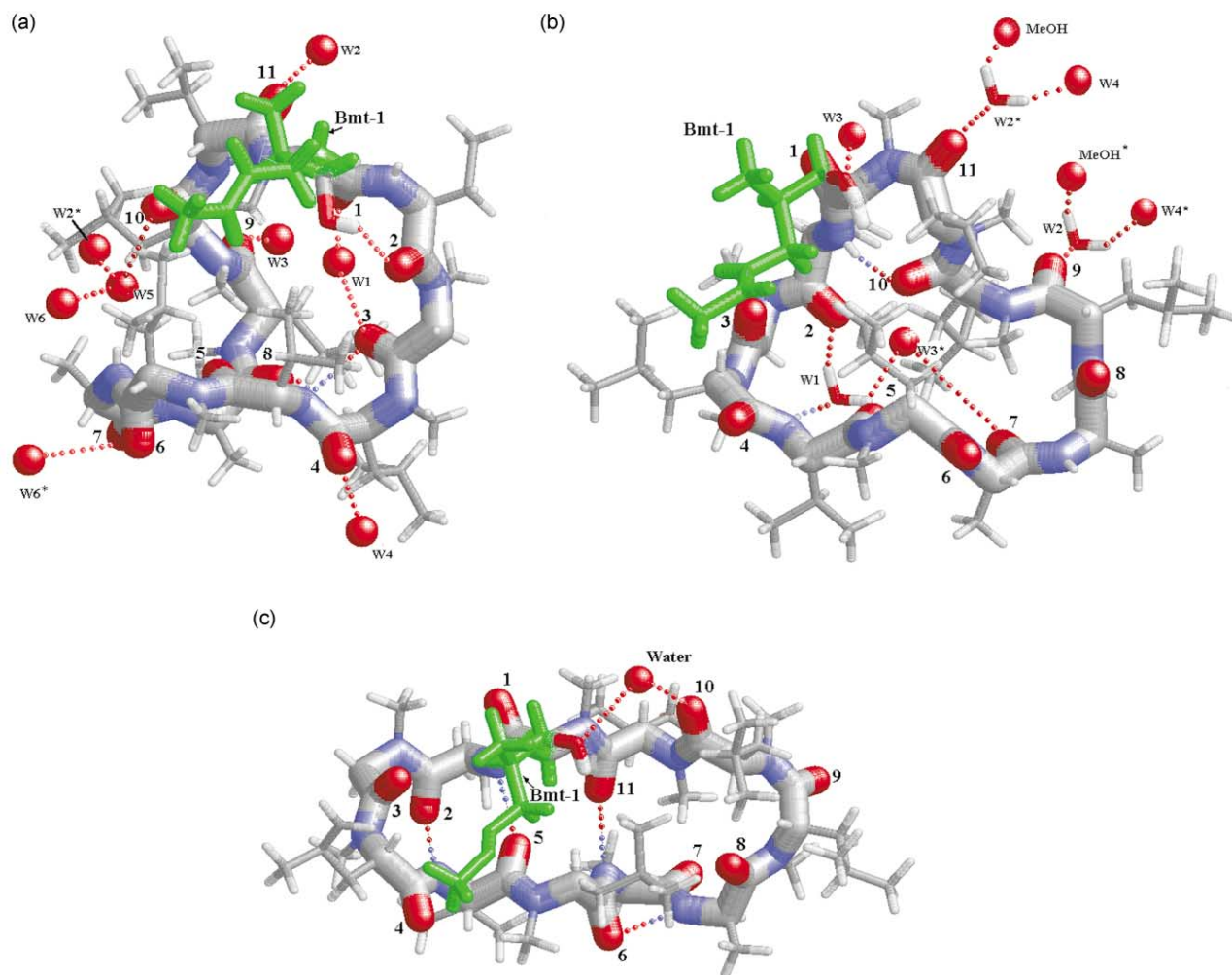


Fig. 1 Secondary structures plotted by RasMol.³² (a) Secondary structure of CsH illustrating the convoluted figure-of-eight folding and water structure. Water 2* is related by symmetry to water 2 and forms a cluster with waters 5 and 6 in CsH form-II. Water 6 occurs only in form-I and links two symmetry-related CsH molecules; waters 1–5 are common to both forms. The hydroxyl of residue MeBmt-1 forms an intramolecular H-bond with L-Abu-2 C=O, *i.e.* O2. (b) Secondary structure of CsG illustrating the compact trefoil folding. Water 1 is highly ordered and plays a significant role in stabilising the molecular conformation, particularly as there are very few direct intra-chain H-bonds. There are two solvent clusters: waters 1 and 3* (symmetry related to 3) and water 2 with both water 4* (symmetry related to 4) and the MeOH* solvate. As water 2* also H-bonds to C=O(11) and water 3 H-bonds to the hydroxyl of residue MeBmt-1, the molecules are strongly associated in the crystal structure. (c) Secondary structure of CsA and principal H-bonds. The water molecule H-bonds to the main chain at residue 10. The pharmacologically important long-chain residue MeBmt-1 stretches across the face of the molecule with its hydroxyl group completing the H-bond bridge to the water molecule. [General notes: H-bonds are shown dotted. Main-chain C=O group numbers are labelled in black. Water and other solvate oxygen atoms are labelled W and coloured red. The main chain radius is 2 × that of Bmt-1 and 3 × those of the remaining 10 side-chains. Bmt-1 is displayed in green to emphasise its important role in cyclosporin function. The sense of the CsA main chain is depicted opposite to those of CsH and CsG (*i.e.* anti-clockwise instead of clockwise), enabling the visibility of Bmt-1 to be optimized].

Comparison of CsA and CsG folding

Very different changes between CsA and CsG, compared to those between CsA and CsH, are observed. The average absolute differences in the main-chain torsion angles between CsA and CsG are 56° in ϕ and 28° in ψ (Fig. 2b and Table 2). A major conformational change in both ϕ and ψ occurs at residue 7; residues 1, 2 and 7 all show changes in ψ greater than 36°; residues 2, 3, 4, 6, 7, 9 and 11 have changes in ψ of at least 24°. A further major difference in main-chain conformation between the CsA structure and CsG occurs at L-MeLeu-9; whereas in CsA^{14,15} the peptide bond geometry is *cis* ($\omega = 3^\circ$), in CsG it is in the usual *trans* conformation ($\omega = -166^\circ$). However in the CsG structure there is a *cis* peptide bond at residue L-MeVal-11, $\omega = 27^\circ$ (178° in CsA^{14,15}). This conformational change in the main chain is closely associated with global structural changes, in particular giving rise to an unusual convex turn between residues 10 and 2 devoid of intra-chain H-bonds (Table 1).

Side-chain conformations in CsH

Table 3 indicates side-chain torsion angles (χ) in the three cyclosporin structures, CsA,^{14,19} CsH and CsG. Torsional degrees of freedom in CsH side-chains are as follows: Abu-2, Val-5 and MeVal-11 each have one; Me-Leu-4, -6, -9 and -10 have two each. All of these side-chains adopt standard conformations. The long, branched MeBmt-1 side-chain has five degrees of freedom and is therefore more susceptible to conformational variations. In CsH form-II this residue is in a highly ordered, partially coiled conformation, whereas in form-I it is subject to bifurcated disordering involving atoms C γ 1, C γ 2, C δ and C ϵ . Side-chain Abu-2 is also disordered in CsH form-I, at C γ . In the X-ray analysis form-I was successfully refined anisotropically, incorporating occupancy factors in addition for the disordered atoms. We assume that Mg(ClO₄)₂ has a stabilising influence on the crystallization of CsH but is not directly incorporated into the crystal structure. The clearer, better resolved electron density for form-II at both room temperature and low temperature

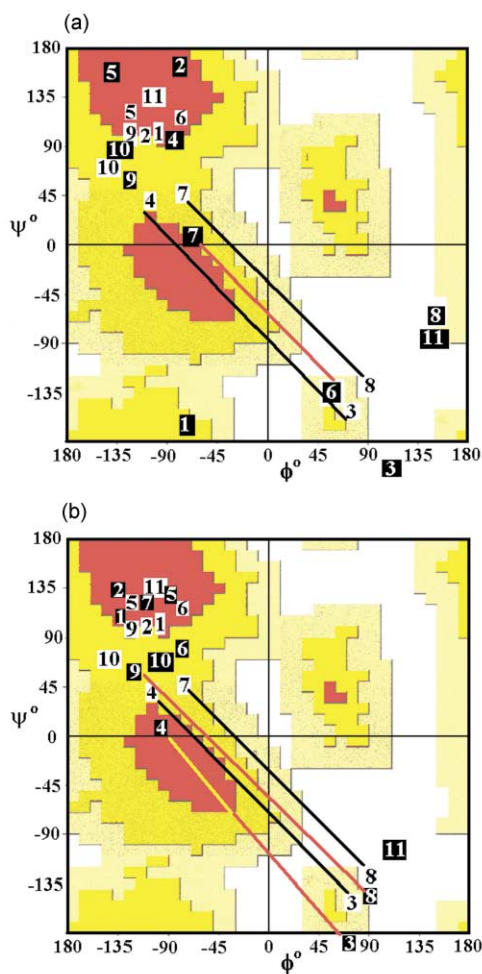


Fig. 2 Composite Ramachandran plots generated using PROCHECK³³ [Note: Conformations are labelled CsH or CsG: white numbers on black background; CsA: black numbers on white background]. (a) Combined plot for CsH and CsA.¹⁴ The greatest change in ϕ , ψ occurs at residue 6 forming part of the open β -sheet in CsA and the apex of a β -turn in CsH. (b) Combined plot for CsG and CsA.¹⁴ The 7–8 γ and 3–4 β -turns in CsA as well as the 3–4 and 8–9 β -turns in CsG are indicated.

is assumed to be a consequence of the stabilising effect of $\text{Mg}(\text{ClO}_4)_2$. The MeBmt-1 side-chain in form-II occupies a single, well-defined location.

Side-chain conformations in CsG

The presence of Nva-2 in CsG instead of Abu-2 in CsA imparts an extra torsional degree of freedom in the side-chain of residue 2. As in CsA and CsH, residues 2, 4–6 and 9–11 are in standard extended conformations. Surprisingly, residue MeBmt-1 shows no disordering in either form of CsG and its partially coiled conformation is very similar to that observed in CsA^{14,19} (Table 1). Side-chain MeLeu-10 is the least ordered in CsG forms I and II, as indicated by slightly larger values for its anisotropic thermal displacement parameters. Form-II crystals give a much better contrast in the diffraction pattern than form-I and it is assumed that, as with CsH, $\text{Mg}(\text{ClO}_4)_2$ has a stabilising influence on the crystallization of CsG whilst not being directly incorporated into the crystal structure.

Molecular surfaces

The classic structure of CsA derived in non-aqueous solution and in a number of single-crystal forms consistently exhibits a closed loop main-chain structure comprising an antiparallel β -sheet, in which four intramolecular H-bonds involving the four non-methylated amide NH groups are preserved.^{14,19} This

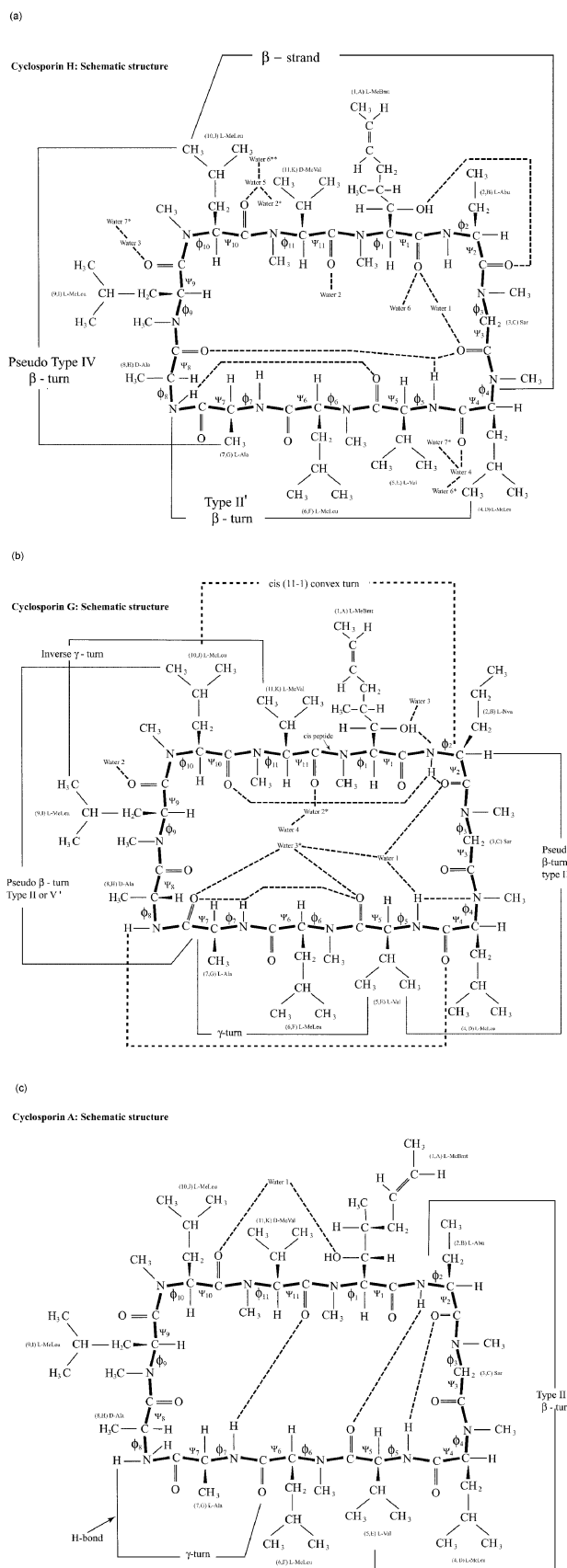


Fig. 3 Secondary structure and hydrogen bonding schemes: (a) CsH, (b) CsG, and (c) CsA. Residues are labelled both 1 to 11 (conventional peptide notation) and A to K (as used in the atom numbering of the crystal structure for refinement). The symbol * indicates a symmetry related atom (usually water) and --- represents a hydrogen bond.

tightly folded arrangement results in a very hydrophobic outer surface (see below). The hydrophobicity of cyclosporins stems largely from the disposition of the various amino acid

Table 1 Three-dimensional secondary structure motifs of the cyclosporins^a

a. Three-dimensional secondary structure motifs of CsA [ref. 19]	
Twisted anti-parallel β -pleated sheet MeVal-11 MeBmt-1 Abu-2 Sar-3 MeLeu-4 Val-5 MeLeu-6 Ala-7 Type-II' β -turn Abu-2 Sar-3 MeLeu-4 Val-5 γ -Turn Ala-7 D-Ala-8 MeLeu-9	
b. Three-dimensional secondary structure motifs and key distances for CsH [corresponding distances for CsA are given in parentheses]	
Single β -strand MeLeu-10 Me-D-Val-11 MeBmt-1 Abu-2 Sar-3 MeLeu-4 Type-II' β -turn Val-5 MeLeu-6 Ala-7 D-Ala-8 Type-IV β -turn Ala-7 D-Ala-8 MeLeu-9 MeLeu-10	Ca5–Ca8 = 5.14/5.15 Å form-I/form-II [8.76 Å] Ca7–Ca10 = 6.10/6.28 Å form-I/form-II [6.50 Å]
c. Three-dimensional secondary structure motifs and key distances for CsG [corresponding distances for CsA are given in parentheses]	
Pseudo type-II' β -turn (convex) Abu-2 Sar-3 MeLeu-4 Val-5 γ -Turn (concave) Val-5 MeLeu-6 Ala-7 Pseudo type-II' or type V' β -turn (convex) Ala-7 D-Ala-8 MeLeu-9 MeLeu-10 Inverse γ -turn (concave) MeLeu-9 MeLeu-10 D-Val-11 <i>cis</i> -Turn (convex) MeLeu-10 D-Val-11 MeBmt-1 Abu-2	Ca2–Ca5 = 8.20/8.21 Å form-I/form-II [5.15 Å] Ca5–Ca7 = 5.70/5.77 Å form-I/form-II [5.68 Å] Ca7–Ca10 = 6.78/6.78 Å form-I/form-II [6.50 Å] Ca9–Ca11 = 4.16/4.16 Å form-I/form-II [6.08 Å] Ca10–Ca2 = 5.13/5.13 Å form-I/form-II [9.38 Å]

^a The term “pseudo” is used to indicate conformations whose torsion angles comply with classic values but where the corresponding H-bonds are absent.

Table 2 Main-chain torsion angles and their differences for CsH–CsA and CsG–CsA pairs, respectively

Residue	ϕ /°			Differences		ψ /°			Differences	
	CsA	CsH	CsG	$\Delta\phi$ CsH–CsA	$\Delta\phi$ CsG–CsA	CsA	CsH	CsG	$\Delta\psi$ CsH–CsA	$\Delta\psi$ CsG–CsA
(1)	–99	–89	–139	10	–40 ^{#a}	103	–174	111	83 [#]	8
(2)	–108	–81	–146	27	–38 [#]	103	165	128	62 [#]	25
(3)	68	95	76	27	8	–136	174	177	–50 [#]	47 [#]
(4)	–106	–95	–117	11	–11	34	99	10	65 [#]	–24
(5)	–110	–141	–119	–31	–9	119	161	129	42 [#]	10
(6)	–86	60	–96	146 [#]	–10	107	–138	82	115 [#]	–25
(7)	–88	–77	–138	11	–50 [#]	51	–3	128	–54 [#]	77 [#]
(8)	83	143	83	60 [#]	0	–127	–76	–133	51 [#]	–6
(9)	–122	–129	–125	–7	–3	102	63	63	–39 [#]	–39 [#]
(10)	–145	–140	–124	5	21	66	81	61	15	–5
(11)	–98	134	–115	–128 [#]	–17	121	–80	84	159 [#]	–37 [#]

^a The most significant differences in corresponding torsion angles are indicated by the # symbol. (e.s.d.'s are in the range 0.4 to 0.6°).

side-chains and must represent a determinant of their biological behaviours. Thus, for example, cyclosporins are soluble in alcohols, chlorinated solvents and ethers but have very poor aqueous solubility. Interestingly, aromatic or polar amino acid groups are absent, and MeBmt-1 alone contains a polar OH group capable of forming intermolecular interactions.

CsH involves two distinct types of side-chain orientation. Residues 1, 5 and 6 (Fig. 1a) protrude in a direction roughly perpendicular to the local molecular surface, while residues 2–4 and 7–11 are located on the opposite side. The convoluted CsH structure therefore forms two predominantly hydrophobic surfaces. In CsA there are again two distinct groups of residues but these are instead oriented on opposite faces of the molecule, residues 1, 4, 6, 10 and 2, 5, 7, 8, 9 and 11 (Fig. 1c). Perhaps more importantly, in CsA the long flexible MeBmt-1 residue may be more amenable to the formation of intermolecular non-polar interactions. In the CsA crystal structure,^{14,19} its orientation is secured initially through hydrogen bonding between the O1 β H group of MeBmt-1 and the lone water molecule, which itself completes a bridge by H-bonding to the main-chain

O10 atom. This anchor serves to orient the long MeBmt-1 side-chain across the face of the CsA molecule towards residue MeLeu-6. However, the MeBmt-1 side-chain in CsH adopts a completely different orientation that is folded securely to the side of the molecule through the H-bond between O1 β H and the main-chain O2 atom. In this folded disposition the ability of the MeBmt-1 side-chain to form intermolecular contacts with the receptor molecule CyP may be less favourable.

In CsG, residues 1, 3, 4, 5, 7, 8 and 9 are lying approximately tangential with respect to the approximate plane of the molecular trefoil surface pointing away from the centre, whilst residues 6 and 10, also tangential, protrude inwards spanning the 1–6 and 6–10 lobes, respectively (Fig. 1b). Residues Nva-2 and MeVal-11 are oriented perpendicular to the trefoil plane, both on the same side of the molecule. The important MeBmt-1 side-chain adopts an orientation approximately parallel to the 1–4 edge of the trefoil and is stabilised through a single H-bond between O1 β H and solvent water 3. Unlike CsA and CsH, the MeBmt-1 side-chain does not link directly or indirectly to the cyclosporin main chain. This is an important

Table 3 Side-chain torsion angles in CsA,¹⁹ CsH and CsG (°)

Residue number	Cs	Amino acid	χ^1	χ^2	χ^3	χ^4	χ^5
1	CsA	MeBmt	-168	77	-178	-128	-178
	CsH		-44	176	-158	26	175
	CsG		179	63	167	-121	-177
2	CsA	Abu	-178	—			
	CsH	Abu	-63	—			
	CsG	Nva	179	173			
4	CsA	MeLeu	-52	-178/-51			
	CsH		-65	161/-77			
	CsG		-52	174/-63			
5	CsA	Val	-174/-51				
	CsH		60/-63				
	CsG		171/-66				
6	CsA	MeLeu	-178	-178/58			
	CsH		-52				
	CsG		-56	-175/-51			
9	CsA ^a	MeLeu	-58	172/-59			
	CsH		-64	162/-71			
	CsG		-66	148/-86			
10	CsA	MeLeu	-165	-167/73			
	CsH		-160	164/-71			
	CsG		-63	175/-59			
11	CsA	MeVal	-178/-51				
	CsH	D-MeVal	173/50				
	CsG ^a	MeVal	-171/-49				

^a *cis* peptide bond. (e.s.d.'s are in the range 0.4 to 0.6°).

feature, which again may influence the pharmacological activity of the drug.

The alterations in structural conformation for CsA, CsG and CsH are evident from their different solvent-accessible surface characteristics, where the presented molecular surfaces (*A*) can be analysed in terms of the component polar and non-polar terms, such that $A = A_p + A_{np}$. Using the analytical method in the GRASP 1.2 programme,²⁴ solvent-accessible surface areas were computed for each unsolvated structure after geometric placement of all H atoms, with standard Lennard-Jones atomic radii and a 1.4 Å probe radius, as detailed previously.²⁵ Surfaces of carbon and carbon-bound hydrogen atoms were defined as non-polar (hydrophobic) and those of all other atoms were classified as polar (hydrophilic).

The CsA structure ($A = 1334 \text{ \AA}^2$, $A_{np} = 1267 \text{ \AA}^2$) presents the least accessible polar surface of the three cyclosporins examined, such that only 5.0% is available for solvent-mediated contact. This situation contrasts markedly with the new crystal structures for both CsG ($A = 1356 \text{ \AA}^2$, $A_{np} = 1257 \text{ \AA}^2$) and CsH ($A = 1319 \text{ \AA}^2$, $A_{np} = 1222 \text{ \AA}^2$), where 7.3% and 7.4% of the total surface can be accessed by a simulated water probe. On this basis, both the CsG and CsH are rather more exposed to favourable intermolecular contacts, and hence more amenable to hydration than the parent CsA derivative. This property indicates that the CsA template may represent a poor basis for rational drug design for cyclosporin-based immunosuppressive agents, in contrast to an earlier suggestion.²⁶

Solvent structure and hydrogen bonding

The presence of hydrogen bonded water molecules in the structures of CsA, CsG and CsH may provide an important rationale for the observed and unexpected large-scale differences in their conformations. CsA includes a single, structurally unimportant water molecule, whereas CsG incorporates a water with important intra-ring H-bonds and a further water and methanol-water cluster. The CsG structures incorporate three solvate oxygen atoms successfully refined as water oxygen atoms and a methanol linked to O2W. In all cases the H-bonding geometry involving solvate oxygen atoms is perfectly acceptable. In the CsG structure (form-I) the solvated O1W molecule is extremely well ordered as judged by

the anisotropic displacement parameters. Consideration of its interactions with neighbouring atoms, however, rules out the possibility that this could be a coordinated Mg^{2+} ion. Future neutron diffraction studies will enable this point to be investigated in more detail by revealing the water H locations, which is not possible with the present X-ray data.

CsH

X-ray data collection from crystals of CsH forms-I and -II was undertaken at room temperature with $\text{CuK}\alpha$ radiation. This enabled the absolute configuration of CsH form-II to be examined by calculating the Flack parameter which depends on Friedel differences in the X-ray intensities. The result (Table 4) is marginally significant and reported here as the first determination of its kind for cyclosporins. The quality of the X-ray data for CsH form-I is inferior to that of form-II because of disorder in some of the side-chains, particularly MeBmt-1, and consequently was processed ignoring Friedel differences. CsH form-II includes seven water molecules forming an extended cluster (Table 4) in the crystal structure. Five of these waters occur in form-I in similar positions, but lack two of the connecting waters (6 and 7). An additional 8th water in form-I only is statistically disordered. Figs. 1(a) and 3(a) show some of the solvent contacts in CsH form-I. The water molecules were assigned from difference electron density calculations and refined, in both forms of CsH, with anisotropic displacement parameters. Water H atoms were fitted geometrically according to H-bond formation and not refined. The very well ordered water 1 is probably the most structurally important water molecule in CsH. It forms an H-bond bridge between main-chain O1 and O3 atoms, O3 also linking across N4H and O8. This strong H-bond network, together with a further H-bond across $\text{O5} \cdots \text{N8H}$, forms the basis of the CsH superstructure. Waters 2, 3, 4, 5 and 6 are less important in this respect. Also of note is the "tethering" of the near end of the MeBmt-1 side-chain *via* H-bonds between O β H to both N2H and O2, thus imposing the location of this side-chain approximately parallel to the main-chain direction. The crystal packing in CsH is dominated by hydrogen bonding involving the water molecules. In form-II main-chain N7H and O1, O3, O4, O9, O10 and O11 all form H-bonds with water molecules. Of the other NH groups and O atoms which are avail-

Table 4 X-ray structure determination statistics for CsH and CsG^a

	CsH	CsG
Molecular formula	C ₆₂ H ₁₁₁ N ₁₁ O ₁₂ ·6.4H ₂ O [C ₆₂ H ₁₁₁ N ₁₁ O ₁₂ ·6H ₂ O]	C ₆₃ H ₁₁₃ N ₁₁ O ₁₂ ·2.4H ₂ O·CH ₃ OH [C ₆₃ H ₁₁₃ N ₁₁ O ₁₂ ·2.4H ₂ O·0.5CH ₃ OH]
Formula weight	1317.92 [1310.71]	1291.92 [1275.90]
Crystal system	Orthorhombic	Orthorhombic
Unit cell dimensions/Å	<i>a</i> = 17.358(2) [17.299(1)] <i>b</i> = 19.515(1) [19.690(1)] <i>c</i> = 23.225(3) [24.137(2)]	12.430(2) [12.3997(2)] 20.256(3) [20.1710(4)] 30.617(4) [30.6428(6)]
Cell volume/Å ³	7867(1) [8221(1)]	7709(2) [7664(2)]
Space group	<i>P</i> 2 ₁ 2 ₁ 2 ₁	<i>P</i> 2 ₁ 2 ₁ 2 ₁
Number of molecules per cell	4	4
Calculated density/g cm ⁻³	1.113 [1.059]	1.126 [1.129]
Solvent molecules	Waters 1–6 and 7 (0.4 occ) [Waters 1–5, 8 all fully occ]	Waters 1–3, Methanol 1
Solvent clusters	1–4–7–3 2–5–6–4 4–6–5–7 [1–4 2–5]	1 + 3, 2 + MeOH
Crystallization conditions	MeOH + Mg(ClO ₄) ₂ , –20 °C [MeOH, –20 °C]	MeOH + Mg(ClO ₄) ₂ , –20 °C [MeOH, –20 °C]
Crystal mounting	Wet in capillary tube	Flash frozen on glass fibre
Diffractometry	<i>ω</i> / <i>θ</i> scans (Nonius CAD4)	<i>φ</i> scans (Nonius CCD plate)
Data collection time	1 min per reflection	90 min [840 min]
Temperature	20 °C	–173 °C
Total number of data	12,266 [18,199]	119,743 [138,783]
Radiation	CuKα <i>λ</i> = 1.54178 Å	MoKα <i>λ</i> = 0.71073 Å
Number of observed data with <i>I</i> > 2σ(<i>I</i>)	11,462 [7278]	6702 [8187]
Rint	0.0339 [0.1752]	0.0745 [0.1752]
Maximum <i>θ</i>	74.61° [69.99°]	24.10° [26.03°]
Resolution ^b	0.80 Å [0.82 Å]	0.87 Å [0.85 Å]
Structure solution, direct methods	SHELXS-86 ²⁹	SHELXS-86 ²⁹
Non-H atoms	Anisotropic ^b	Anisotropic ^b
H-atoms (riding for Cs atoms and fixed for solvate atoms)	Isotropic	Isotropic
Structure refinement, full-matrix least-squares	SHELXL-97 ³⁰	SHELXL-97 ³⁰
Data/restraints/parameters	11,462/0/911 [7278/1292/993]	6702/0/905 [8187/30/901]
Precision (bond lengths)	0.0035 Å [0.0045 Å]	0.0035 Å [0.0055 Å]
Precision (bond angles)	0.20° [0.35°]	0.20° [0.45°]
Flack parameter	–0.4(2)	
Absolute configuration determined	Yes [No]	No [No]
Residual <i>R</i> 1	0.0582 [0.0892]	0.0558 [0.0661]
<i>w</i> <i>R</i> 2 (all data)	0.1555 [0.2418]	0.1485 [0.1813]
Largest difference + and – e Å ⁻³	0.34, –0.16 [0.61, –0.28]	0.40, –0.20 [0.42, –0.23]
Goodness-of-fit on <i>F</i> ²	0.964 [1.060]	1.042 [1.008]

^a Data are for crystal form-II. Crystal data for form-I are given in parentheses where there is a significant difference compared to form-II. ^b All water oxygens and non-H methanol atoms were refined anisotropically. Where stated some solvate molecules were assigned partial occupancy on the basis of an independent refinement run. ^c In the room temperature structure CsH I the long side-chain 1 (L-Bmt) is almost entirely disordered and was modelled in two distinct parts, refined with occupancies 0.58208 and (1 – 0.58208) respectively. The end of side-chain 4 (L-Me-Leu) is also disordered with occupancies 0.28854 and (1 – 0.28854). These disordered regions are absent in CsH II ex Mg(ClO₄)₂ which consequently refines to a much better structure. Both low temperature CsG structures refine well and are devoid of disorder except for statistical disorder in one of the waters in both structures and the methanol solvate in CsG I.

able for H-bond formation, O2, N5, O5, and N8 are satisfied, leaving only O6 and O7 without H-bonds.

In comparison, the crystal structure of CsA^{14,19} includes a single solvated water molecule H-bonded to three sites: (1) O10 of residue MeLeu-10; (2) the side-chain oxygen of residue MeBmt-1; and (3) a symmetry related oxygen O9' in residue MeLeu-9. All of these sites are hydrated in CsH, but with three distinct water molecules. It is somewhat surprising that CsA contains a single water molecule H-bonded to the peptide main chain and the OH group of side-chain 1, while CsH has seven waters participating in both intra- and intermolecular interactions. Both CsA and CsH were crystallized from non-aqueous media (acetone and MeOH, respectively). It is therefore a point for conjecture as to when hydration of the molecules may have taken place.

No evidence of ordered solvated Mg(ClO₄)₂ was found in CsH form-II, although crystals subjected to X-ray fluorescence measurements produced strong signals for both Mg and Cl. Similarly, the Raman spectrum (not shown) gives an intense signal due to the perchlorate ion, even when the incident beam is focused within the crystal, but no evidence of ordering.

CsG

X-ray data collection from both forms of CsG crystals was undertaken at liquid N temperature with MoKα radiation. This technique produced very good quality measurements within a short total exposure time, which was necessary in view of the possibility of crystal instability if exposed to X-rays for longer periods, but the use of Mo radiation precludes the determination of absolute configuration. Like CsH, CsG is more highly solvated than CsA, there being three water molecules and one methanol, which forms an H-bond cluster to water 2 in both forms (Fig. 3b). All solvate molecules were refined successfully with anisotropic thermal displacement factors, and H atoms were attached geometrically and fixed. In form-I the methanol is statistically disordered and was assigned an occupancy factor of 0.5. Water 3, also statistically disordered and assigned an occupancy factor of 0.4 in both forms, nevertheless forms well-defined H-bond bridges between main-chain O7, O5 and water OW1 (Fig. 3b), and thus contributes to the overall stability of the molecule. Waters 1 and 2 are both highly ordered as judged by their anisotropic thermal parameters. Water 2 forms an H-bond to main-chain O10 and links to a symmetry related

CsG molecule in the crystal structures of both forms. Water 1 is perhaps the most important solvent molecule as it forms stabilising H-bonds to main-chain O2 and N4H atoms, as well as linking to O5 and O7 *via* water 3. Other notable intramolecular H-bonds contributing to the CsG secondary structure are those between main-chain atoms, N2H \cdots O10 and N7H \cdots O5. As in the case of CsH, but to a lesser extent, the crystal packing in CsG is dominated by hydrogen bonding involving the water molecules. Main-chain atoms N5H, and O2, O5, O7, O11 and side-chain O12 (in MeBmt-1) all form H-bonds to water molecules. Unlike the CsH structure, packing in CsH also involves a main-chain to main-chain interaction, namely N8H \cdots O4* (* indicates a symmetry related position) and a side-chain to main-chain interaction between O12H and O7*. Main-chain atoms O1, O3, O6 and O8 do not participate in H-bond formation.

Discussion

The high resolution structures determined for both CsH and CsG provide the first conformational details of these two cyclic peptides. The observed, and unexpected, conformations of CsH and CsG offer a basis to explain their significant differences in pharmacological activity compared to the "standard" cyclosporin drug CsA. Global structural differences in terms of conformation and polar/non-polar surface topology are manifest for the outwardly similar therapeutic agents. On this basis, the present study illustrates the value of high-resolution crystallography in rational structure-driven drug design strategies. CsA, the best characterised and medically most widely used member of the cyclosporin family, is believed to exist as multiple conformers in aqueous solution.²⁷ It is remarkable therefore that to date only one accurate structure for CsA itself has been reported¹⁹ and this is far less precise than the structures for CsH and CsG reported here. Recently,²⁸ a high-resolution structure of a supposed *synthetic* form of CsH, obtained by acid degradation of CsA as starting material, was published. Detailed examination of this structure reveals that it is very similar to the classic CsA structure with a single solvated water molecule. This is in contrast to the structure of the *natural form* of CsH presented here which is heavily solvated and in addition displays a unique conformation which bears no resemblance to the known CsA folding or the synthetic CsH folding. Furthermore no evidence is presented in this paper²⁸ that the material used is actually CsH in terms of its biological activity.

It is possible, however, in view of the relative *chemical* differences between CsA, CsG and CsH that the novel conformations we describe could be mimicked by CsA itself and form part of its repertoire of structural variations required to explain its biological properties, including, for example, its recently reported²⁷ temperature-dependent membrane permeability. Whilst this remains to be demonstrated, the present results provide the basis for such studies to be initiated. The determination of ultra high-resolution structures for biologically relevant molecules and/or their molecular complexes continues to pose a pivotal challenge. This goal is critical from the viewpoint of probing structure–function linkages in terms of molecular recognition and dynamics, as well as understanding the kinetics and thermodynamics of receptor–ligand interactions. Such data will be essential for the *de novo* design of biologically relevant ligands and improved or "tailored" next-generation therapeutic agents with receptor specificities that can be predicted from structural considerations.

Experimental

Highly purified cyclosporin samples were supplied by Sandoz-Novartis (Basle, Switzerland).

Crystallization and data collection

Crystals of CsH form-I were grown over 21 days at $-20\text{ }^{\circ}\text{C}$ from MeOH in partially sealed glass vials. Crystals of form-II, which are isomorphous with form-I, were grown under identical conditions but in the presence of $\text{Mg}(\text{ClO}_4)_2$. This was observed to improve the quality of the X-ray diffraction pattern and to have a stabilising effect on the structure, especially the long MeBmt-1 side-chain, which is considerably disordered in the absence of $\text{Mg}(\text{ClO}_4)_2$. The crystals are approximately $1.0 \times 0.5 \times 0.3\text{ mm}^3$, disintegrate spontaneously on exposure to air, and were mounted rapidly in glass capillary tubes for data collection. X-ray data were collected with $\text{CuK}\alpha$ radiation, $\lambda = 1.54178\text{ \AA}$, on a Nonius CAD4 diffractometer at room temperature. Crystals were stable during the course of data collection. Flash frozen crystals of both CsH forms were also subjected to X-ray analysis at $-150\text{ }^{\circ}\text{C}$ using $\text{MoK}\alpha$ radiation, $\lambda = 0.71073\text{ \AA}$. The success of these experiments enabled the techniques required for handling CsG crystals, which do not diffract significantly at room temperature, to be developed. Isomorphous crystals of CsG, forms I and II, were grown under similar conditions to those for CsH. The presence of $\text{Mg}(\text{ClO}_4)_2$ in form-II stabilises the MeVal-11 side-chain and dramatically improves the diffracting power both at room temperature and at $-150\text{ }^{\circ}\text{C}$. Unlike CsH form-I, the long MeBmt-1 side-chain is well ordered in both forms of CsG. The crystals are again at least $1.0 \times 0.5 \times 0.3\text{ mm}^3$ with good morphology, but disintegrate spontaneously on exposure to air. Even when mounted rapidly in glass capillary tubes, CsG crystals diffract extremely poorly at room temperature and require cooling to $-150\text{ }^{\circ}\text{C}$ for X-ray analysis. Data were collected from flash frozen crystals using synchrotron radiation, $\lambda = 0.6885\text{ \AA}$, on station 9.8 at the CLRC Laboratory (Daresbury, UK), and with $\text{MoK}\alpha$ radiation, $\lambda = 0.71073\text{ \AA}$ at the SERC Service (Department of Chemistry, University of Southampton, Southampton, UK) using Bruker and Nonius CCD image plates respectively. Crystals were stable during the course of data collection. The CsG structure was initially determined with synchrotron data and then refined against low temperature $\text{MoK}\alpha$ data. Crystal data for both CsH and CsG are given in Table 4. ‡

Structure determination and refinement

The structures of CsH and CsG were solved by direct methods using the SHELXS-86²⁹ programme and refined using SHELXL-97³⁰ implemented in the WinGX system of programs.³¹ Non-hydrogen atoms were refined anisotropically by full-matrix least-squares techniques. Hydrogen atom positions were calculated geometrically and refined in riding mode with isotropic displacement parameters common for all H's attached to the same carbon atom. In each CsH structure, six hydrate atoms were refined as water oxygen atoms and show acceptable H-bonding geometries.

Geometrical calculations were also made in WinGX. Figs. 1(a), (b) and (c) were prepared using RasMol³² and Figs. 2(a) and (b) are derived from PROCHECK³³ plots.

Acknowledgements

We thank the CLRC Laboratory, Daresbury, UK for use of the synchrotron X-ray facility station 9.8, and the SERC X-ray service (Department of Chemistry, University of Southampton, UK) for use of X-ray facilities. Sandoz-Novartis (Basle, Switzerland) is thanked for the highly purified cyclosporin samples. Financial support was provided by the DevR RAE fund of the University of Greenwich (to BZC and RW)

‡ CCDC reference numbers 195320–195323. See <http://www.rsc.org/suppdata/ob/b2/b210086j/> for crystallographic files in .cif or other electronic format.

and Yorkshire Cancer Research (to TCJ). RW and BZC are grateful to the EPSRC for the award of a grant (GR/L85176) for the purchase of the Labram Raman spectrometer. Fig. 3 was produced by Effective Graphics.

References

- 1 C. B. Carpenter, *N. Eng. J. Med.*, 2000, **342**, 647–648.
- 2 J. F. Borel, F. Dipadova, J. Mason, V. Quesniaux, B. Ryffel and R. Wenger, *Pharmacol. Rev.*, 1989, **41**, 239–434.
- 3 J. F. Borel, Z. L. Kis and T. Beveridge, The history of the discovery and development of cyclosporine (Sandimmune), 1985 [in: *The Search for Anti-Inflammatory Drugs* (V. J. Merluzzi & J. Adams, eds.), pp. 27–63, Birkhäuser, Boston].
- 4 Y. Theriault, T. M. Logan, R. Meadows, L. P. Yu, E. T. Olejniczak, T. F. Holzman, R. L. Simmer and S. W. Fesik, *Nature*, 1993, **361**, 88–91.
- 5 P. Teofoli, O. DePita and T. M. Lotti, *Skin Pharmacol.*, 1997, **10**, 79–84.
- 6 G. Baumann, G. Zenke, R. Wenger, P. Hiestand, V. Quesniaux, E. Andersen and M. H. Schreier, *J. Autoimmun.*, 1992, **5**, 67–72.
- 7 J. Liu, *Immunol. Today*, 1993, **14**, 290–295.
- 8 D. A. Fruman, S. J. Burakoff and B. E. Bierer, Molecular actions of cyclosporin A, FK506 and rapamycin, 1994; [in: *Immunosuppressive Drugs. Developments in Anti-Rejection Therapy* (A. W. Thomson & E. Starzl, eds.), pp. 14–35, Arnold, London].
- 9 C. Weber, G. Wider, B. von Freyberg, R. Traber, W. Braun, H. Widmer and K. Wüthrich, *Biochemistry*, 1991, **30**, 6563–6574.
- 10 D. Altschuh, O. Vix, B. Rees and J.-C. Thierry, *Science*, 1992, **256**, 92–94.
- 11 J. Kallen, V. Mikol, P. Taylor and M. D. Walkinshaw, *J. Mol. Biol.*, 1998, **283**, 435–449.
- 12 V. Mikol, P. Taylor and M. D. Walkinshaw, *J. Mol. Biol.*, 1998, **283**, 451–461.
- 13 S.-K. Ko and C. Dalvit, *Int. J. Pept. Protein Res.*, 1992, **40**, 380–382.
- 14 H.-R. Loosli, H. Kessler, H. Oschkinat, H. P. Weber, T. J. Petcher and A. Widmer, *Helv. Chim. Acta*, 1985, **68**, 682–704.
- 15 H. Kessler, M. Kock, T. Wein and M. Gehrke, *Helv. Chim. Acta*, 1990, **73**, 1818–1832.
- 16 S. W. Fesik, R. T. Gampe, H. L. Eaton, G. Gemmecker, E. T. Olejniczak, P. Neri, T. F. Holzman, D. A. Egan, R. Edalji, R. Simmer, R. Helfrich, J. Hochlowski and M. Jackson, *Biochemistry*, 1991, **30**, 6574–6583.
- 17 K. Wüthrich, B. von Freyberg, C. Weber, G. Wider, R. Traber, H. Widmer and W. Braun, *Science*, 1991, **254**, 953–954.
- 18 S. W. Fesik, P. Neri, R. Meadows, E. T. Olejniczak and G. A. Gemmecker, *J. Am. Chem. Soc.*, 1992, **114**, 3165–3166.
- 19 R. B. Knott, J. Schefer and B. P. Schoenborn, *Acta Crystallogr., Sect. C*, 1990, **46**, 1528–1533.
- 20 K. WenzelSiefert, C. M. Hurt and R. Seifert, *J. Biol. Chem.*, 1998, **273**, 24181–24189.
- 21 K. Kitegaki, H. Nagai, S. Hayashi and T. Totsuka, *Eur. J. Pharmacol.*, 1997, **337**, 283–289.
- 22 H. Muhl, D. Kunz, P. Rob and J. Pfeilschrift, *Eur. J. Pharmacol.*, 1993, **249**, 95–100.
- 23 B. E. Bierer, *Prog. Clin. Biol. Res.*, 1994, **390**, 203–223.
- 24 A. Nicholls, K. Sharp and B. Honig, *Proteins: Struct., Funct., Genet.*, 1991, **11**, 281–296.
- 25 I. Haq, L. E. Ladbury, B. Z. Chowdhry, T. C. Jenkins and J. B. Chaires, *J. Mol. Biol.*, 1997, **271**, 244–257.
- 26 M. D. Walkinshaw, H.-P. Weber and A. Widmer, *Triangle*, 1986, **25**, 131–142.
- 27 P. F. Augustijns, S. J. Brown, D. H. Willard, T. G. Consler, P. P. Annaert, R. W. Hendren and T. W. Bradshaw, *Biochemistry-US*, 2000, **39**(25), 7621–7630.
- 28 A. Jegorov, L. Cvak, A. Husek, P. Šimek, A. Heydová, J. Ondráček, S. Pakhomova, M. Hušák, B. Kratochvíl, P. Sedmera and V. Havlíček, *Collect. Czech. Chem. Commun.*, 2000, **65**, 1317–1328.
- 29 G. M. Sheldrick, 1986. *SHELXS-86: Program for the solution of crystal structures*, University of Göttingen, Germany.
- 30 G. M. Sheldrick, 1997. *SHELXL-97: Program for the refinement of crystal structures*, University of Göttingen, Germany.
- 31 L. J. Farrugia, *J. Appl. Crystallogr.*, 1998, **32**, 837–838.
- 32 R. Sayle, 1994. *RasMol: A Molecular Visualisation Program*, Glaxo, Greenford, Middlesex, UK.
- 33 R. A. Laskowski, M. W. MacArthur, D. S. Moss and J. M. Thornton, *J. Appl. Crystallogr.*, 1993, **26**, 283–291.